

Connectivity-Based Joint Parameter Estimation in One-Dimensional Wireless Sensor Networks

(Invited Paper)

Nour Zaarour
EMT Centre
INRS
Montreal, Canada
nour.zaarour@emt.inrs.ca

Sofiène Affes
EMT Centre
INRS
Montreal, Canada
affes@emt.inrs.ca

Nahi Kandil
School of Engineering
UQAT
Rouyn-Noranda, Canada
nahi.kandil@uqat.ca

Nadir Hakem
School of Engineering
UQAT
Rouyn-Noranda, Canada
nadir.hakem@uqat.ca

Abstract—In this paper, we propose a novel joint estimation scheme for the range, path-loss exponent (PLE), and inter-node distances based on the received signal strength (RSS) and the network’s information of an anchor-less (i.e., without anchor nodes) curvilinear wireless sensor network (CLWSN). Assuming a random node distribution along a one-dimensional curve (e.g., in deployments over gas/oil/water pipelines, railway tracks, underground mine tunnels, subway networks, city sewage networks, street/road lights, etc.), and adopting a propagation model that combines both large-scale PLE and log-Normal shadowing, we derive new analytical expressions for the node’s communication range as a function of the network’s connectivity and density and for the PLE as a function of the node’s range and both the network’s connectivity and density. Once we calculate the node’s range and the PLE, we estimate all distances between nodes using an RSS-based method. We illustrate by simulations the superior accuracy of our new joint range, PLE, and distance estimation technique against state-of-the-art benchmarks in terms of the normalized mean absolute error (NMAE). We thereby highlight the major contributions of this work by demonstrating both: i) the ability of our new solution to jointly estimate the node’s range, the PLE, and all inter-node distances with relatively high accuracy using solely the RSS and network’s connectivity and density; and ii) its significant potential for enabling very cost-effective yet highly accurate positioning over anchor-less (e.g., in GPS-denied harsh environments) wireless sensor networks (WSNs).

Index Terms—Wireless sensor network (WSN), curvilinear WSN (CLWSN), anchor-less WSN, log-Normal shadowing, received signal strength (RSS), connectivity, density, joint estimation, communication range, path-loss exponent (PLE), inter-node distances.

I. INTRODUCTION

Low-cost, small-size, and low-power multi-functional sensor nodes that communicate over short distances have been recently designed and developed to take advantage of advances in wireless communications and digital electronics [1]. Capabilities of these nodes in sensing, data processing, and communication allow the implementation of WSNs. The

This work was supported by the DG and CREATE PERSWADE <www.create-perswade.ca> Programs of NSERC, a Discovery Accelerator Supplement Award from NSERC, and the Collaborative RD (CRD) Grants Program of NSERC, Bell Aliant, and Newtrax.

strength of a WSN does not stem from the potential of a single device, but from the ability of all its nodes to collaborate.

In this work, we consider a new subclass of WSNs, the curvilinear or one-dimensional WSN known as CLWSN that is emerging today as a major focus area of research. In CLWSNs nodes are deployed along one or more lines in a strictly linear or semi-linear form. Due to this special topology, issues and solutions are different from those arising in and required for an ordinary WSN [16]. This type of network is progressively finding wider use in many applications. Indeed, CLWSNs are extremely relevant and useful in the monitoring of underground environments [17], railway tracks [18], oil, gas or water pipelines [19], and so forth. In such application examples where security inspection is critical, deployments could stretch over lines of tens to thousands of kilometers long, making manual monitoring a daunting, time-consuming, and costly task. However, introduction of CLWSNs makes automation of inspection and control, remotely and almost instantly on demand, a viable and economical option [16]. Many more application examples can be listed. For the sake of conciseness, we limit the discussion to the compelling use-cases already mentioned above and adopt more generically WSN¹ instead of CLWSN in the remainder of the paper.

Inter-node distances estimation in WSNs is necessary and fundamental in that it offers a physical context to sensor readings. Indeed, location information is fundamental for services such as intrusion detection, surveillance, geographic routing, and coverage area management [2]. Common measurements used for localizing nodes in WSNs are the RSS [3], time of arrival (TOA) [4], time difference of arrival (TDoA) [5], angle of arrival (AoA) [6], or combinations thereof. Whereas range-free methods do not require the latter and rather exploit the radio-communication connectivity established between nodes [1]. RSS-based methods are ideal for low-cost and low-complexity networks, since no additional hardware is needed.

¹Possible extensions to 2D or 3D network topologies, beyond the scope of this contribution, are currently under investigation and will be addressed in future publications.

However, the exact knowledge of the propagation model is of greatest importance for RSS-based localization or ranging.

The PLE, γ , is one of the key parameters that could properly characterize large-scale propagation over wireless fading channels. Indeed, it has a major impact on the node's communication range and RSS interpretation. Hence, calibration is essential for the estimation of some key parameters such as the PLE whose accuracy has significant effects on ranging or localization performance. Many studies have exploited different channel parameter and node position estimates. In [7], the authors assumed the PLE to be known a priori and developed a maximum likelihood (ML) or linear least square (LLS) estimator to localize nodes [8], whereas others relied on channel measurements between nodes to localize them [9]. In [10], the authors proposed a weighted least square (WLS) estimator for the sensor positions that accounts for some uncertainty model over the PLE. So and Lin devised in [11] an LLS estimator for RSS-based positioning. Whereas, Wang et al. in [12] derived a weighted LLS formulation to jointly estimate the PLE and node locations. In [13], the authors assumed the PLE to be random then obtained it with Bayesian MMSE before deriving a general nonlinear equation for ML distance estimation. In [14], the authors proposed a generalized total least square algorithm (GTLS) for RSS-based localization with unknown path-loss model parameters.

However, to the best of our knowledge, no joint range, PLE, and distance estimation technique exists so far in the open literature that would rely mainly on a key yet simple and already available feature of WSNs, namely its connectivity information; and what is more, in the absence of anchor nodes. Anchors are more costly than regular nodes and their deployment in WSNs is very often a complicated manual task. Besides, estimation performance will suffer greatly if some of the anchors accidentally break down, even if the remaining ones continue to function. Hence, it is highly desirable to rid as much possible WSNs from their dependence on anchors so as to reduce hardware cost, power consumption, communication overhead, and deployment complexity [15]. Therefore, a new joint estimation solution that could operate accurately over anchor-less WSNs with such multiple benefits should offer a significant progress of and contribution to the current state-of-the-art.

In this paper, we develop a novel approach that jointly estimates the range, the PLE, and inter-node distances over anchor-less WSNs by making use of the under-exploited yet invaluable network connectivity data. Simulation results unambiguously show the superior accuracy of our new joint range, PLE, and distance estimation technique against state-of-the-art benchmarks in terms of NMAE. They also demonstrate its ability to execute this joint estimation task accurately using solely the RSS and network's connectivity and density; and its significant potential for enabling very cost-effective yet highly accurate positioning over anchor-less WSNs.

The remainder of this paper is organized as follows: We formulate the problem in section II. In section III, we propose a novel approach for jointly estimating the range, the PLE and

all inter-node distances over anchor-less WSNs. We discuss our simulation results in section IV before drawing out our concluding remarks in section V.

II. ASSUMPTIONS AND WSN MODEL

Consider a curvilinear WSN consisting of N nodes placed randomly at positions x_i for $i = 1, \dots, N$ along the deployment curve segment $[x_{min} \ x_{max}]$ [i.e., with node density $\lambda = N/(x_{min} \ x_{max})$] and having transmission ranges R_i for $i = 1, \dots, N$ (i.e., a heterogeneous WSN a priori) assumed in this work to be unknown. This topology is well-justified in environments that impose one-dimensional deployments such as narrow-vein underground mines [20], [21], sewage or water distribution networks, subway tunnels, etc. In wireless communications, the received signal power in dBm is modeled as the sum of large-scale path-loss and log-Normal shadowing. The basic and well-known log-distance path-loss model in [22] quantifies the amount of large-scale variations in different propagation environments. The received power P_{rij} at node i of a signal emitted from node j is modeled by [22] as

$$P_{rij}(d_{ij}) = P_r(d_0) - 10 \gamma \log_{10} \left(\frac{d_{ij}}{d_0} \right) + X_\sigma, \quad (1)$$

where $P_r(d_0)$ is the received power from any given node (given the fact that we assume that all nodes are tuned a priori to transmit data with the same power level) at the reference distance $d_0 = 1$ (predicted from the Friis free space propagation loss model [22]), γ is the PLE with common values ranging between 2 and 6, d_{ij} is the distance separating the two nodes i and j , and X_σ is the large-scale log-Normal shadowing with variance σ^2 acting here as an unknown additive Gaussian white noise. The received power matrix can then be defined as

$$\mathcal{P}_r = [P_{rij}]_{N \times N}. \quad (2)$$

III. PROPOSED CONNECTIVITY-BASED JOINT ESTIMATION

Our proposed approach, divided into three parts, consists in estimating the range, the PLE, and then the inter-node distances. We assume that propagation conditions remain the same in the area where the WSN is deployed (i.e., path-loss and shadowing have the same statistics). We also assume a fully-connected network, i.e., information can be transmitted between any two sensors in the network following the shortest multi-hop path covered by the minimum number of hops possible.

To deal with PLE estimation, we must estimate the communication range R as a function of the nodes' connectivity and density information. Based on [23], a homogeneous Poisson process is adopted. The nearest neighbor method known from analysis of spatial data [24] is employed to estimate each node's communication range, then the PLE. An enhanced RSS-based method is ultimately applied to estimate inter-node distances.

A. Connectivity Information

Connectivity information can be obtained by comparing the received power at any node against a minimum detection threshold P_{th} . Two nodes are neighbors at one hop if they are connected according to the following random variable definition

$$C_{ij} = \begin{cases} 1 & \text{if } P_{rij} \geq P_{th} \\ 0 & \text{if } P_{rij} < P_{th} \end{cases}, \quad (3)$$

for $i = 1, \dots, N$ and $j = 1, \dots, N$ with $i \neq j$. Hence, $C_{ij} = 1$ if the distance separating the receive node i and transmit node j , d_{ij} , is less or equal to the communication range of node j , i.e., $d_{ij} \leq R_j$. Otherwise, $C_{ij} = 0$ and, hence, the nodes i and j are far apart and node j cannot communicate with node i directly without the help of some intermediate nodes. The network connectivity matrix \mathcal{C} is then defined as

$$\mathcal{C} = [C_{ij}]_{N \times N}. \quad (4)$$

B. Range Estimation

Due to space limitation, we will consider in this work a homogeneous Poisson point process (PPP) in one dimension, where N nodes are randomly positioned over the interval $[x_{min} \ x_{max}]$. Extensions to two- or three-dimensional WSNs, far from being ad hoc, go far beyond the scope of this contribution, but will be soon considered in future works.

Let the random variable n denote the number of nodes within a given interval $[x_l \ x_r]$. The probability that a node falls within the interval $[x_l \ x_r]$ is $p = \frac{x_r - x_l}{x_{max} - x_{min}}$. From [23], the probability that v nodes out of N fall within the interval $[x_l \ x_r]$ is

$$P(n = v) = \binom{N}{v} p^v (1 - p)^{N-v}, \quad (5)$$

and can be approximated by a Poisson distribution as

$$P(n = v) = \frac{(Np)^v}{v!} e^{-Np}. \quad (6)$$

For a given density λ , the probability that v nodes fall within the interval $[x_{min} \ x_{max}]$ of length $x_0 (x_0 = x_r - x_l)$ is given by:

$$P(n = v) = \frac{(\lambda x_0)^v}{v!} e^{-\lambda x_0}. \quad (7)$$

The average number of neighbor nodes falling within a radius $\frac{x_0}{2}$ around a given node i can be calculated as

$$\bar{n}_i = E(n_i) = \lambda x_0. \quad (8)$$

For a given node i with a communication range R_i , the expected number of connected neighbor nodes can be then calculated as

$$\bar{n}_i = E(n_i) = 2R_i \lambda. \quad (9)$$

Hence, the average number of connected neighbors per node is

$$\bar{n} = E(\bar{n}_i) = \frac{1}{N} \sum_{i=1}^N \bar{n}_i = 2\lambda \frac{1}{N} \sum_{i=1}^N R_i = 2\bar{R}\lambda, \quad (10)$$

where \bar{R} is the average communication range over all nodes, a fortiori unknown as well.

Furthermore, n_i , the number of connected neighbors to node $i = 1, \dots, N$, can be estimated from the connectivity data as

$$\hat{n}_i = \sum_{j=1}^N C_{ij}. \quad (11)$$

From (9) and (11), we can estimate the range R_i of node i as

$$\hat{R}_i = \frac{1}{2\lambda} \sum_{j=1}^N C_{ij}. \quad (12)$$

Hence, the average number of connected neighbors per node can be estimated as

$$\hat{\bar{n}} = \frac{1}{N} \sum_{i=1}^N \hat{n}_i = \frac{1}{N} \sum_{i=1}^N \sum_{j=1}^N C_{ij}. \quad (13)$$

From (10) and (13), we can estimate the average range \bar{R} as

$$\hat{\bar{R}} = \frac{1}{2\lambda} \sum_{i=1}^N \frac{\hat{R}_i}{N} = \frac{1}{2\lambda N} \sum_{i=1}^N \sum_{j=1}^N C_{ij} = \frac{\hat{\bar{n}}}{2\lambda}. \quad (14)$$

C. PLE Estimation

From the large-scale path-loss model in (1), we can estimate the PLE γ by assuming that the received power from a transmit node at another – it is connected to – is equal to the power detection threshold P_{th} when the distance separating them is equal to the estimated average range \hat{R}_i in (12). Hence, the PLE estimate can be obtained as

$$\hat{\gamma}_i = \frac{-P_{th} + P_r(d_0)}{10 \log_{10}(\hat{R}_i)}, \quad (15)$$

or preferably over the whole WSN as

$$\hat{\gamma} = \frac{1}{N} \sum_{i=1}^N \hat{\gamma}_i. \quad (16)$$

Please note in the particular homogeneous WSN case, where all nodes are a priori known to have the same communication range (i.e., $R_i = \bar{R}$ for $i = 1, \dots, N$), that the PLE can be estimated using the average-range estimate as

$$\hat{\gamma} = \frac{-P_{th} + P_r(d_0)}{10 \log_{10}(\hat{\bar{R}})}. \quad (17)$$

D. Distance Estimation

Each node i , for $i = 1, \dots, N$, estimates its distances to its connected neighbor nodes $k \neq i \in \zeta_i = \{i_1, \dots, i_{\hat{n}_i}\}$ as

$$\hat{d}_{ik} = 10^{\frac{P_r(d_0) - P_{rik}}{10 \hat{\gamma}}}, \quad (18)$$

where ζ_i represents the set of neighbors to node i , and P_{rik} is the received power at node i from node k .

Algorithm 1 RANGE, PLE, AND DISTANCE ESTIMATION ALGORITHM.

\mathcal{C} : is the connectivity matrix
 \mathcal{P}_r : is the received power matrix
Input N : is the number of nodes

For $i \leftarrow 1$ to N
 For $j \leftarrow 1$ to N
 $\mathcal{P}_r \leftarrow$ using (2)
 $\mathcal{C}_{ij} \leftarrow$ using (3)
 $\mathcal{C} \leftarrow$ using (4)
 End

End
For $i \leftarrow 1$ to N
 $\hat{n}_i \leftarrow$ using (11)
End

$\hat{n} \leftarrow$ using (13)
 $\hat{R} \leftarrow$ using (14)
 $\hat{\gamma}_i \leftarrow$ using (15)
 $\hat{\gamma} \leftarrow$ using (16) or (17)
For $i \leftarrow 1$ to N
 $\hat{d}_{ik} \leftarrow$ using (18)
End

E. Relative Positioning

As mentioned previously in Section I, our joint parameter estimation technique is an anchor-less solution that addresses, in general, a fundamental problem: the recovery of the WSN's key propagation characteristics and geometry mainly from the connectivity information. In fact, instead of computing the absolute node positions, it can estimate the relative positions with respect to a coordinate system established by a reference group of nodes [25], since these locations stem immediately from distance estimation. Relative positioning can be satisfactory and work efficiently in many applications such as location-aided routing [26] as one example. Moreover, a relative coordinate system can still be transformed into an absolute coordinate system by just including a single anchor node serving as a reference point.

IV. SIMULATION RESULTS

In this section, we conduct extensive simulations to evaluate the performance of our new joint estimation solution for the range, the PLE, and the distance using MATLAB. We also compare it with some of the most representative benchmarks available in the literature, but only for distance estimation. Indeed, to the best of our knowledge, none tackles the estimation of all three parameters jointly. To do so, we consider a multi-hop linear WSN of N nodes deployed for the sake of simplicity in a homogeneous environment, i.e., all nodes have a priori the same communication range $R_i = \bar{R}$ for $i = 1, \dots, N$ with density λ along a segment of length $x_{max} - x_{min}$. Performance results are assessed over N_{MC} random topologies or Monte-Carlo runs. RSS measurements are generated using the path-loss model in (1). As mentioned in section III, we assume a fully-connected network, i.e.,

TABLE I: WSN SIMULATION PARAMETERS SETUP

| Parameter [Unit] | Value(s) |
|--|---------------------|
| γ : PLE | [2.5; 3; 3.5; 5; 5] |
| N : WSN node's number | 65 |
| λ : WSN density [node/m] | 1/3 |
| σ : Log-Normal shadowing standard deviation [dB] | [1; 2; 3; 4; 5; 6] |
| $(x_{max} - x_{min})$: Deployment distance [m] | 200 |
| $P_r(d_0)$: Received power at reference $d_0 = 1$ [dBm] | -45 |
| P_{th} : Threshold power [dBm] | -90 |
| N_{MC} : Number of tested Monte-Carlo topologies | 1000 |

information can be transmitted through an existing multi-hop path between any two sensors in the network. All relevant WSN simulation parameters are listed in Table I. Since our solution is able to jointly estimate three parameters, namely, the average range \bar{R} , the PLE γ , and all inter-node distances d_{ik} , we adopt in all our assessments and comparisons below the NMAE [27], [28] as our key performance metric for all three estimators of these parameters.

A. Range Estimation

As mentioned in section II, the communication range R , in our study is unknown. However, we can calculate its nominal value R using (1) as

$$R = 10^{\frac{[P_r(d_0) - P_{th}]}{10 \gamma}}, \quad (19)$$

by assuming that the received power becomes equal to the threshold value P_{th} , when the distance separating two nodes is equal to the communication range. Table II lists the values of R obtained for typical values of the PLE when the received power at the reference distance $d_0 = 1$ is set to -45 dBm.

TABLE II: AVERAGE-RANGE VALUES VERSUS THE PLE.

| γ | 2.5 | 3 | 3.5 | 4 | 5 |
|----------|-------|-------|-------|-------|------|
| R [m] | 63.09 | 31.60 | 19.30 | 13.30 | 7.94 |

To evaluate the efficiency of our method in the estimation of the average range using (14), we assess its NMAE as

$$\epsilon_{\bar{R}} = E_{MC} \left[\frac{|\hat{\bar{R}} - \bar{R}|}{\bar{R}} \right], \quad (20)$$

where E_{MC} denotes averaging over all Monte-Carlo runs. We also define the range's NMAE as

$$\epsilon_R = E_{MC} \left[\frac{1}{N} \sum_{i=1}^N \frac{|\hat{R}_i - R_i|}{R_i} \right]. \quad (21)$$

The red curves in Fig. 1 plot the range's NMAE versus σ , the log-Normal shadowing standard deviation, for the different PLE values listed in Tab. II. As expected, errors increase both with σ and γ (i.e., more severe path-loss and log-Normal shadowing). The lowest and highest values of 0.19 and 0.32 are reported when the couple of channel parameters (γ, σ) is set to (2.5, 1) and (5, 6), respectively. At high values of σ , the NMAE curves tend to converge to about the same level of errors for all values of γ larger than or equal to 3. On the other

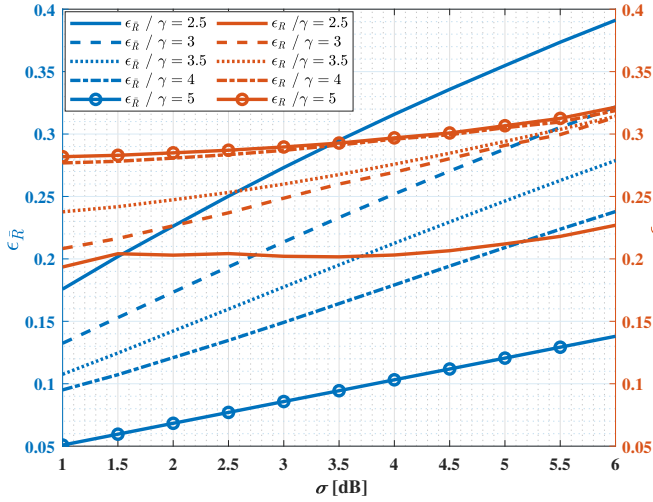


Fig. 1: Average-range NMAE and range NMAE vs. the log-Normal shadowing standard deviation for different PLE values.

hand, the blue curves in Fig. 1 plot the average-range's NMAE versus σ for the same PLE values. As expected, errors increase with σ (i.e., more severe log-Normal shadowing) for any given value of γ . However, against all intuitive expectations, errors decrease on the contrary with γ (i.e., more severe path-loss) for any given value of σ . The lowest and highest values of 0.05 and 0.39 are reported when the couple of channel parameters (γ, σ) is set to $(5, 1)$ and $(2.5, 6)$, respectively. This is due to the fact that smaller PLE values translate into higher average-range values. The latter increases from about 8 to 63 meters when the PLE value decreases from 5 to 2.5, respectively. As such, the number of neighbors within range, yet at more than a single-hop distance, becomes increasingly larger thereby biasing more severely the estimate in (14). Nevertheless, the average-range estimates (i.e., blue curves) remain in most cases (except for $\gamma = 2.5$ and σ larger than 1.5 and $\gamma = 3$ and σ larger than 5.5) far more accurate than the per-node range estimates (i.e., red curves). This shows the advantage of knowing a priori that a WSN is homogeneous, i.e., when the average-range estimate can replace the range estimate at each node, more so at smaller values of σ and larger values of γ .

B. PLE Estimation

To assess the performance of our solution in the estimation of the average PLE, we define its NMAE as

$$\epsilon_{\bar{\gamma}} = E_{MC} \left[\frac{|\hat{\bar{\gamma}} - \bar{\gamma}|}{\bar{\gamma}} \right]. \quad (22)$$

We also define the PLE's NMAE as

$$\epsilon_{\gamma} = E_{MC} \left[\frac{1}{N} \sum_{i=1}^N \frac{|\hat{\gamma}_i - \gamma_i|}{\gamma_i} \right]. \quad (23)$$

The red curves in Fig. 2 plot the PLE's NMAE versus σ , the log-Normal shadowing standard deviation, for the PLE values

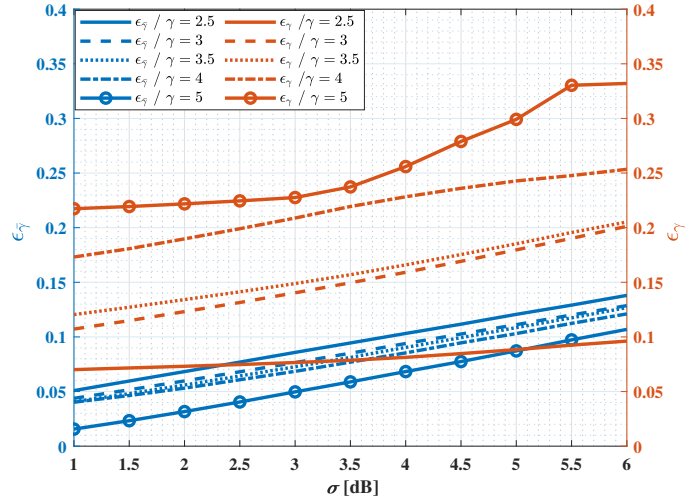


Fig. 2: Average-PLE NMAE and PLE NMAE vs. the log-Normal shadowing standard deviation for different PLE values.

listed in Tab II. As expected once again, errors increase both with σ and γ . The lowest and highest values of 0.07 and 0.35 are reported when the couple of channel parameters (γ, σ) is set to $(2.5, 1)$ and $(5, 6)$, respectively. On the other hand, the blue curves plot the average-PLE's NMAE versus σ . Again as expected, errors increase with both σ for any given value of γ . However, once more, against all intuitive expectations as in Fig. 1 with the average range, errors decrease on the contrary with γ for any given value of σ . The lowest and highest values of 0.07 and 0.35 are reported when the couple of channel parameters (γ, σ) is set to $(2.5, 1)$ and $(5, 6)$, respectively. This is hardly surprising since estimation of the average PLE in (17) stems directly from the estimation of the average range in (14). However, once again the average-PLE estimates (i.e., blue curves) remain in most cases (except for $\gamma = 2.5$ and σ larger than 2.4) far more accurate than the per-node PLE estimates (i.e., red curves). This shows once again the advantage of knowing a priori that a WSN is homogeneous, more so at smaller values of σ and larger values of γ .

C. Distance Estimation

In order to prove the efficiency of the proposed technique in terms of distance estimation accuracy, we gauge its NMAE performance against best representative benchmarks available in the literature. Explicitly, we consider the weighted least square (WLS) [10], the linear least square (LLS) [11], and generalized total least square (GTLS) [14] methods. The distance NMAE, ϵ_d , is defined as

$$\epsilon_d = E_{MC} \left[\frac{1}{N} \sum_{i=1}^N \frac{1}{\mathcal{S}(\zeta_i)} \sum_{k \in \zeta_i} \frac{|\hat{d}_{ik} - d_{ik}|}{d_{ik}} \right], \quad (24)$$

where $\mathcal{S}(\zeta_i)$ is the size or the cardinal of ζ_i , the set of node- i 's neighbors. In Fig. 3, we assess it versus the log-Normal shadowing for different PLE values in two different scenarios

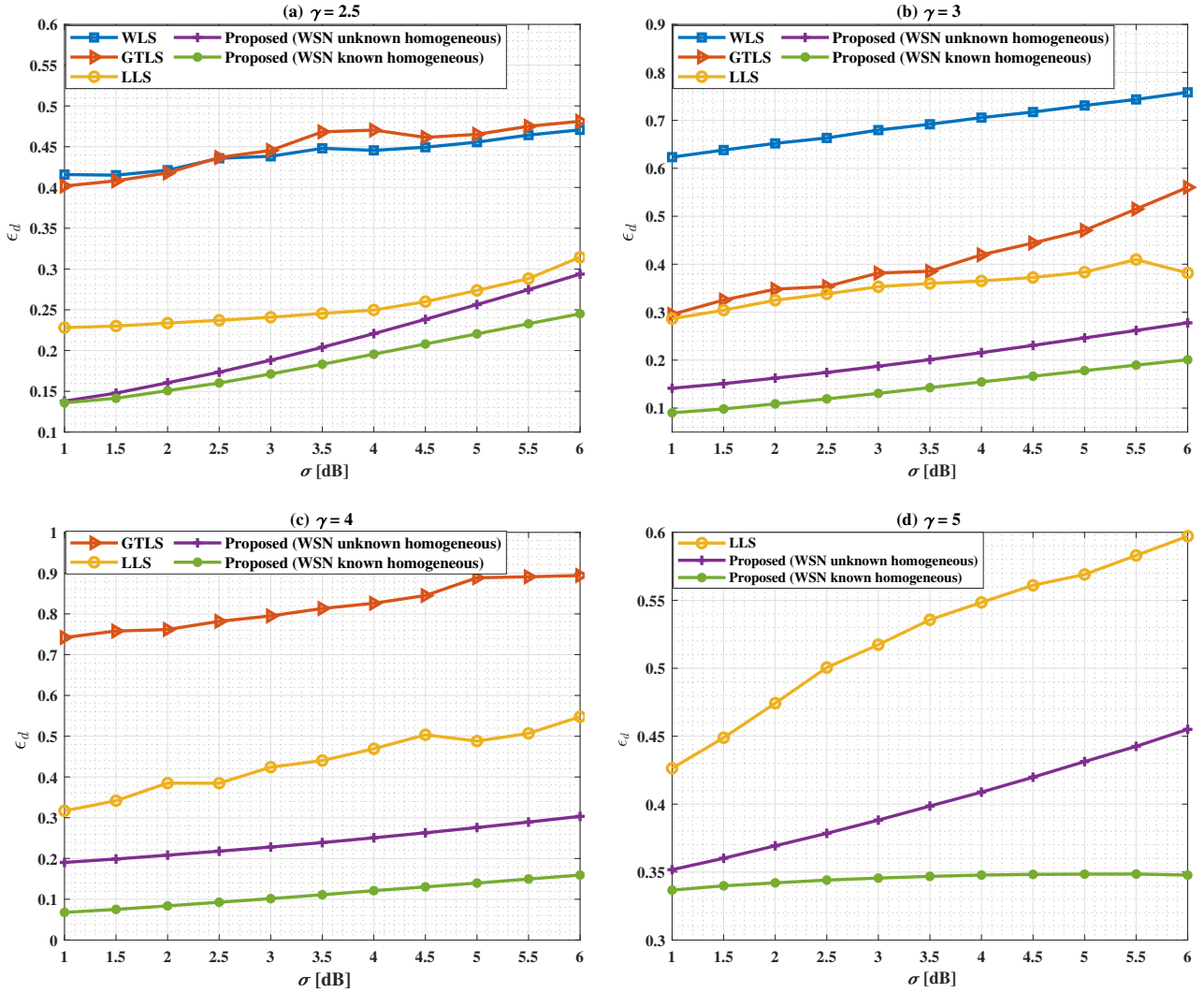


Fig. 3: Distance NMAE vs. the log-Normal shadowing standard deviation for different PLE values

where we assume the homogeneity of the WSN to be either known (i.e., possible exploitation of the average-range and average-PLE estimates) or unknown (i.e., exploitation of the per-node range and PLE estimates). First of all, we observe that the proposed estimator outperforms all benchmarks no matter the values of σ and γ . However, as the PLE increases from 2.5 to 5 in Figs. 3 (a) to (d), the accuracy gain of the new anchor-less estimator over the anchor-based benchmarks increases as the latter keep deteriorating more and more severely, in contrast to the proposed solution that is far more robust to the PLE and the log-Normal shadowing. At $\gamma = 4$, WLS can no longer work and is removed from Fig. 3 (c). Whereas GTLS collapses at $\gamma = 5$ and is removed from Fig. 3 (d). More importantly, we observe that the proposed estimator with the a priori knowledge of the network homogeneity outperforms the one without that prior information, more so at larger values of σ and γ . Both see their accuracy decrease with σ . However, the latter sees its performance deteriorate

with γ whereas the former shows the opposite trend (except for the extreme PLE value of 5).

V. CONCLUSION

In this paper, we proposed a novel joint estimation scheme for the range, PLE, and inter-node distances of an anchor-less WSN based on its connectivity data and the RSS. To do so, we have been able to derive new analytical expressions for both the per-node and average communication range and the PLE. From there, we have been able to estimate all distances between nodes using an RSS-based approach. Comparisons through extensive simulations with best representative anchor-based benchmarks show the superior accuracy of our new approach. Our solution was derived for one-dimensional WSNs that find today wider use in many new applications. However, extensions to two- or three-dimensional network topologies are under investigation and will be the very soon subject of future disclosures.

REFERENCES

- [1] I.F. Akyildiz and M. Can Vuran, *Wireless Sensor Networks*. John Wiley Sons Ltd, 2010.
- [2] W. Dargie and C. Poellabauer, *Fundamentals of Wireless Sensor Networks Theory and Practice*. John Wiley Sons Ltd, 2010.
- [3] O.G. Adewumi, K. Djouani, and A.M. Kurien, "RSSI Based Indoor and Outdoor Distance Estimation for Localization in WSN," in *Proc. IEEE Int. Conf. ICIT*, Cape Town, South Africa, 2013, pp. 1534–1539.
- [4] S. Hong, D. Zhi, S. Dasgupta, and Z. Chunming, "Multiple Source Localization in Wireless Sensor Networks Based on Time of Arrival Measurement," *IEEE Trans. Signal Process.*, vol. 62, no. 8, pp. 1938–1949, Feb. 2014.
- [5] W. Meng, L. Xie, and W. Xiao, "Decentralized TDOA Sensor Pairing in Multihop Wireless Sensor Networks," *IEEE Signal Process. Lett.*, vol. 20, no. 2, pp. 181–184, Feb. 2013.
- [6] H.J. Shao, X.P. Zhang, and Z. Wang, "Efficient Closed-Form Algorithms for AOA Based Self-Localization of Sensor Nodes Using Auxiliary Variables," *IEEE Trans. Signal Process.*, vol. 62, no. 10, pp. 2580–2594, May 2014.
- [7] S.D. Chitte, S. Dasgupta, and Z. Ding, "Distance Estimation from Received Signal Strength Under Log-Normal Shadowing: Bias and Variance," *IEEE Signal Process Lett.*, vol. 16, no. 3, pp. 216–218, Mar 2009.
- [8] R. Ouyang, A.S. Wong, and C.T. Lea, "Received Signal Strength-Based Wireless Localization via Semi-Definite Programming: Non-Cooperative and Cooperative Schemes," *IEEE Trans. Vehic. Technol.*, vol. 59, no. 3, pp. 1307–1318, Mar. 2010.
- [9] G. Mao, B.D.O. Anderson, and B. Fidan, "Path-loss Exponent Estimation for Wireless Sensor Network Localization," *Computer Network*, vol. 51, no. 10, pp. 2467–2483, July 2007.
- [10] D. Li and J. Huang, "RSS Based Method for Sensor Localization with Unknown Transmit Power and Uncertainty in Path-loss Exponent," *8th IEEE ICCSN*, Beijing, China, 2016, pp. 298–302.
- [11] H.C. So and L. Lin, "Linear Least Squares Approach for Accurate Received Signal Strength-Based Source Localization," *IEEE Trans. Signal Process.*, vol. 59, no. 8, pp. 4035–4040, Aug. 2011.
- [12] W. Gang, H. Chen, L. Youming, and J. Ming, "On Received-Signal-Strength Based Localization with Unknown Transmit Power and Path-loss Exponent," *IEEE Wirel. Commun. Lett.*, vol. 1, no. 5, pp. 536–539, Oct. 2012.
- [13] R. Sari and H. Zayyani, "RSS Localization Using Unknown Statistical Path-loss Exponent Model," *IEEE Commun. Lett.*, vol. 22, no. 9, pp. 1830–1833, Sep. 2018.
- [14] G. Rahimi, M.R. Danaee, and S. Bayat, "A Generalized Total Least Squares Algorithm for RSS-Based Localization with Unknown Path-loss Model Parameters," in *24th ICEE*, Shiraz, Iran, 2016, pp. 521–524.
- [21] K. Shah and D. C. Jinwala, "A Secure Expansive Aggregation in Wireless Sensor Networks for Linear Infrastructure," in *Proc. of IEEE Region 10 Symposium (TENSYP)*, Bali, Indonesia, 2016, pp. 207–212.
- [15] A.K. Paul and T. Sato, "Localization in Wireless Sensor Networks: A Survey on Algorithms, Measurement Techniques, Applications and Challenges," *J. Sens. Actuator Network*, vol. 6, issue 4, Oct. 2017.
- [16] S. Varshney, K. Chiranjeev, and S. Abhishek, "Linear sensor networks: Applications, Issues and Major Research Trends," in *Int. Conf. on Computing, Communication Automation*, Noida, India, 2015, pp. 446–451.
- [17] N. Mohamed, I. Jawhar, J. Al-Jaroodi, and L. Zhang, "Monitoring Underwater Pipelines Using Sensor Networks", in *Proc. of 12th IEEE Int. Conf. on High Performance Computing and Communications*, Melbourne, VIC, Australia, 2010, pp. 346–353.
- [18] F. Stajano, N. Hault, I. Wassell, P. Bennett, C. Middleton, and K. Soga, "Smart Bridges Smart Tunnels: Transforming Wireless Sensor Networks from Research Prototypes into Robust Engineering Infrastructure," *Ad Hoc Networks*, vol. 8, issue 8, pp. 872–888, Nov. 2010.
- [19] Z. Sun, P. Wang, M.C. Vuran, M.A. Al-Rodhaan, A. M. Al-Dhelaan, and I.F. Akyildiz, "BorderSense: Border Patrol Through Advanced Wireless Sensor Networks", *Ad Hoc Networks*, vol. 9, issue 3, pp. 468–477, May 2011.
- [20] B. Yu, W. Yuanping, Z. Liang, H. Yuan, and Z. Aijuan, "Relay Node Deployment for Wireless Sensor Networks Based on PSO," in *Proc. of 2015 IEEE Int. Conference on Computer and Information*, Liverpool, United Kingdom, 2015, pp. 2393–2398.
- [22] T.S. Rappaport, *Wireless Communications*. New Jersey: Prentice Hall, 1999.
- [23] C. Bettstetter, "On the Minimum Node Degree and Connectivity of a Wireless Multihop Network," in *Proc. of the 3rd ACM Int. Symp. Mobile Ad Hoc Netw. Comp. (MobiHoc)*, Lausanne, Switzerland, 2002, pp. 80–91.
- [24] N.A.C. Cressie, *Statistics for Spatial Data*. John Wiley Sons, 1991.
- [25] A. Youssef, A. Agrawala, and M. Younis, "Accurate Anchor-Free Node Localization in Wireless Sensor Networks," in *Proc. of 24th IEEE Int. Performance, Computing, and Communications Conference*, Phoenix, AZ, USA, 2005, pp. 465–470.
- [26] K. Singh, A. Sharma, and N.K. Singh, "Linear Regression Based Energy Aware Location-Aided Routing Protocol for Mobile Ad-Hoc Networks," in *Int. Conf. on Computational Intelligence and Communication Networks (CICN)*, Jabalpur, India, 2015, pp. 114–121
- [27] H. Bilil, H. Gharavi, "MMSE-Based Analytical Estimator for Uncertain Power System with Limited Number of Measurements," *IEEE Trans. Power Syst.*, vol. 33, no. 5, pp. 5236–5247, Sep. 2018.
- [28] T.K. Reddy, V. Arora, S. Kumar, L. Behera, Y. Wang, and C. Lin, "Electroencephalogram Based Reaction Time Prediction with Differential Phase Synchrony Representations Using Co-Operative Multi-Task Deep Neural Networks," *IEEE Trans. on Emerging Topics in Computational Intelligence*, vol. 3, no. 5, pp. 369–379, Oct. 2019.